2024 IEEE/RSJ International Conference on Intelligent Robots and Systems (IROS)
October 14-18, 2024. Abu Dhabi, UAE

Contact Stability Control of Stepping Over Partial Footholds Using Plantar Tactile Feedback

J. Rogelio Guadarrama-Olvera[1], Shuuji Kajita[2], Fumio Kanehiro[3] and Gordon Cheng[1]

***Abstract*— This work presents a novel method to keep stable contact and balance while stepping over partial footholds for biped humanoid robots with flat feet. We exploit plantar tactile feedback to detect the geometry of the terrain and reconstruct online the new supporting polygon after landing every step. Plantar tactile feedback detects early contacts to stop the swing foot motion. Then we compute the convex hull of the cluster of contact points detected by distributed normal force sensors over the foot soles. The centroid of the supporting polygon is then used for retargeting the reference ZMP and DCM positions. Finally, the supporting polygon is used to define constraints for ZMP balance feedback control. These methods were implemented in two biped humanoid robots running different walking controllers.**

I. INTRODUCTION

The pursuit of humanoid robots capable of navigating complex and unstructured environments has long been a driving force in robotics research. Achieving stable locomotion for biped robots in such scenarios remains challenging due to the inherent difficulties associated with foot placement and balance control. A skill that considerably increases the range of possible terrains for biped locomotion is the capability of stepping over partial footholds while walking (i.e., the footholds that are smaller than the sole of the robot's feet). Stepping over partial footholds requires a robot capable of detecting the partial foothold when the swing leg lands a new step. After identifying the terrain condition, the walking motions must be adjusted to keep the postural stability by distributing the ground reaction forces over the small foothold.

This letter presents methods to directly introduce plantar tactile feedback to detect the partial footholds and define kinematic constraints for balance feedback control that allow keeping the walking motions stable while stepping over partial footholds. These advances were added into two different walking controllers, the Model Predictive Control (MPC)-based Linear Inverted Pendulum Model (LIPM) tracking control [1] and the Divergent Component of Motion (DCM) based walking controller [2]. These controllers were run in an HRP-2 Kai robot [3] and the H1 robot [4] shown in Fig. 1.

[1] J. Rogelio Guadarrama Olvera and G. Cheng are with the Institute for Cognitive Systems, Technical University of Munich, Arcisstrae 21, 80333 Munich, Germany. rogelio.guadarrama@tum.de, gordon@tum.de

[2]S. Kajita is with the Dept. of Robotic Science and Technology, Chubu University, 1200 Matsumoto-cho, Kasugai-shi, Aichi, 487-8501 Japan. shuuji.kajita@fsc.chubu.ac.jp

[3]F. Kanehiro is with the CNRS-AIST Joint Robotics Laboratory (JRL), IRL, National Institute of Advanced Industrial Science and Technology (AIST), Tsukuba, Ibaraki 305-8560, Japan. f-kanehiro@aist.go.jp

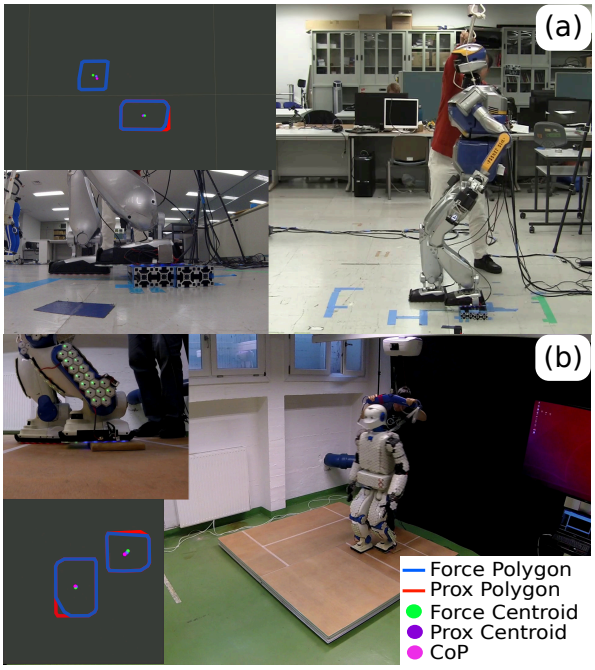

Fig. 1: Experimental platforms used to evaluate the proposed improvements for walking control. a) the HRP-2 Kai robot [3] running the QP based walking controller [1]. b) the H1 robot [4] running the DCM based walking controller [2].

A. Walking over partial footholds.

The most common premise to define foothold contact constraints is that all the foot sole has a fixed contact with the ground, as highlighted by Caron et al. [6]. This assumption is explicitly stated in several works on biped balance and walking control as [7]–[9] due to the lack of a precise method to find the actual support polygon online.

When the footholds are smaller than the sole, the supporting polygon can be estimated with exploratory motions as in [10] or with the reaction produced by the foot tilting over the terrain as proposed by Wiedebach et al. [11]. However, exploratory motions drastically slow down the walking movement, and letting the robot tilt over the terrain requires fast reactions to recover before losing the balance, which may not be realizable in robots with large reduction gearboxes.

Previous knowledge of the terrain can allow planning footsteps that consider partial footholds as shown in [12]. Nevertheless, a full scan of the environment is computationally expensive and may be affected by occlusions. Another

method to detect partial footholds is by including additional sensors in the robot foot to acquire information about the terrain. For example, mounting contact switches on the corners of the sole helps detect early contacts and allows walking over partial footholds, as shown in [13]. Nevertheless, early contact detection adapts the foot orientation to find other fixation points on the terrain rather than to stabilize the supporting contact.

B. Plantar robot skin for terrain feedback.

As introduced in previous works [14], [15], plantar tactile feedback provides an approximated shape of the supporting polygon right after the foot lands on the ground. Furthermore, with plantar proximity sensing, a preemptive shape of the next foothold can be acquired in advance during the last part of the swing leg motion. The geometric information of the contact is available immediately after the foot landing with no need for exploratory movements, which allows replan the step if the terrain condition is not safe, or as will be explored in this work, to adapt the walking patterns online to step over the small foothold keeping a stable contact.

C. Contributions

In this work, the geometric information provided by plantar robot skin is used to improve walking and balance control over partial footholds as follows:

- When the robot detects a partial foothold while landing a new step, it adjusts the reference position for the Zero Moment Point (ZMP) to the centroid of the supporting polygon. Consequently, the reference waypoints for the DCM are updated as well.
- The bounding box of the supporting polygon is used to rewrite the friction constraints introduced by Caron et al. [6] to guarantee contact stability when stepping over a partial foothold.
- The measured supporting polygon allows removing the full-sole contact assumption in the DCM-ZMP chained balance control by constraining the adjustments of the desired ZMP proposed by Engelsberger et al. [2].

II. PLANTAR TACTILE FEEDBACK

The formulations in the following sections are designed for a biped robot with plantar skin with the following features:

- The soles of the robot are fully covered by skin.
- The position and shape of all the taxels (the units of our skin sensor) in the skin are known.
- The taxels of one foot must not saturate when holding the whole robot's weight.
- The taxels provide force sensing modality.
- Full tactile information must be provided at a rate suitable for the walking controller running in the robot.

A. Ground reaction forces and ZMP

In a set of k taxels mounted on a sole with a coordinate frame $\boldsymbol{O}_{sole}$ located at the sole surface, the i-th taxel measures the contact force $\boldsymbol{f}_{F,i} = [f_{F,i,x}\ f_{F,i,y}\ f_{F,i,z}]^\top \in \mathbb{R}^3$ at its mounting coordinate frame $\boldsymbol{O}_i$. Assuming a spatially calibrated robot skin, the transformation ${}^{sole}\boldsymbol{T}_i$ from $\boldsymbol{O}_i$ to the sole coordinate frame $\boldsymbol{O}_{sole}$ is known and composed by the rotation ${}^{sole}\boldsymbol{R}_i \in SO(3)$ and the translation ${}^{sole}\boldsymbol{t}_i \in \mathbb{R}^3$. These parameters are illustrated in Fig. 2.

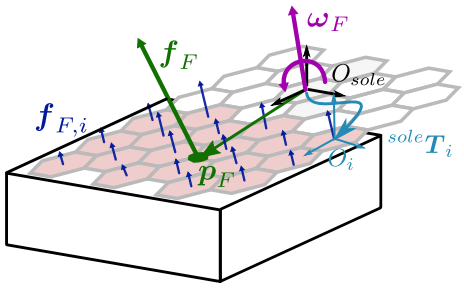

Fig. 2: Ground reaction forces measured from plantar robot skin.

Considering the contribution of all the taxels on the sole, the resultant ground reaction wrench (GRW) at $\boldsymbol{O}_{sole}$ frame is calculated as

$$\boldsymbol{\omega}_F = \begin{bmatrix} \boldsymbol{f}_F \\ \boldsymbol{\tau}_F \end{bmatrix} = \sum_{i=1}^{k} \begin{bmatrix} {}^{sole}\boldsymbol{R}_i\, \boldsymbol{f}_{F,i} \\ {}^{sole}\boldsymbol{t}_i \times {}^{sole}\boldsymbol{R}_i\, \boldsymbol{f}_{F,i} \end{bmatrix} \in \mathbb{R}^6, \quad (1)$$

where $\boldsymbol{f}_F = [f_{F,x}\ f_{F,y}\ f_{F,z}]^\top$ is the GRF, and $\boldsymbol{\tau}_F = [\tau_{F,x}\ \tau_{F,y}\ \tau_{F,z}]^\top$ the ground reaction torque (GRT), both in $\boldsymbol{O}_{sole}$ coordinate frame. This is equivalent to the measurement of a 6D force-torque sensor mounted at $\boldsymbol{O}_{sole}$. Furthermore, with this information and assuming no offset between $\boldsymbol{O}_{sole}$ and the ground, the ZMP of the contact between the sole and the ground can be estimated as

$$\boldsymbol{p}_{sole} = \begin{bmatrix} \frac{-\tau_{sole,y}}{f_{sole,z}} & \frac{\tau_{sole,x}}{f_{sole,z}} & 0 \end{bmatrix}^\top \quad (2)$$

B. Supporting polygon

As presented in [14], every time a sole gets in contact with the ground, a subset of the taxels will sense the ground and provide the information to estimate the shape of the contact. The process to construct the supporting polygon is described in Fig. 3. The real contact area S_{real} can be approximated from the known geometry of the taxels, which detect a contact force $||\boldsymbol{f}_{F,i}|| > \epsilon_t$. The contours of these taxels generate a cluster $S_{cluster}$ whose convex hull S_F approximates the supporting polygon encapsulating S_{real}. The accuracy of S_F is inversely proportional to the size of the taxels. The convex hull of the cluster of points $S_F \subset \mathbb{R}^3$ can be obtained from different algorithms as described in [16]. For the case of flat feet, $S_F := \{\boldsymbol{\phi} \subset \mathbb{R}^3 \mid \phi_z = 0\}$. Note that $\epsilon_t > 0 \in \mathbb{R}$ is a threshold value defined to discard noise and to make the iteration over all the set of taxels faster by skipping the taxels with a small force detected.

For control purposes, a simplified convex polygon can be generated using iterative algorithms such as [17] to find the maximum area inscribed triangle inside a convex polygon, [18] to find the maximum area inscribed parallelogram inside a convex polygon, or [19] for finding the minimal area enclosing parallelogram containing a cluster of points. These

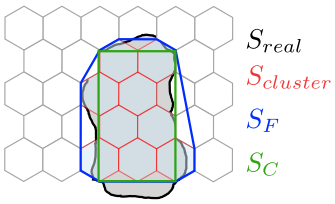

Fig. 3: Supporting polygon constructed from tactile information. The real contact geometry S_{real} can be approximated. from a cluster $S_{cluster}$ with the contours of the skin that detects contact. The convex hull S_F approximates the supporting polygon. This information can be used to define contact constraints as the quadrilateral S_C.

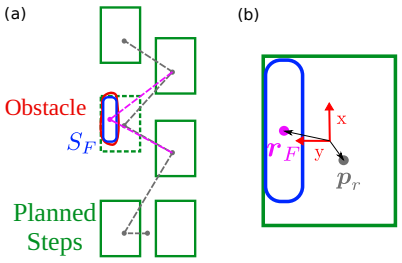

Fig. 4: Reference ZMP adjustment from tactile information when a foot lands over a foothold smaller than the sole.

polygons will be used in Section III to define constraints for the balance controllers.

III. WALKING CONTROL WITH PLANTAR TACTILE FEEDBACK

Motion planning for bipedal robot walking starts by planning the footsteps over the terrain. Then, a feasible reference ZMP trajectory must be defined within these footsteps. A usual strategy is to assign the ZMP waypoints at the center of the planned steps where full-sole contact is assumed. Finally, a smooth trajectory for the center of mass is defined using a simplified model such as the LIPM. Nevertheless, during the execution of the motion, disturbances and uncertainties make the system deviate from the plan, and feedback control is required to track the reference trajectories. Therefore, the trajectories should be continuously adjusted from sensor feedback whenever a foot lands a new step. This applies in the case of a foot landing over a partial foothold. However, plantar tactile information can help re-plan the walking motion as described in Fig. 4.

As described in Section II, plantar robot skin provides an approximation of the real contact geometry and, thus, the supporting polygon. Additionally, the centroid of a convex polygon can be easily computed with fast algorithms as [20]. The centroid of the supporting polygon r_F can be used as an immediate new reference position for the ZMP right after contact is detected, as shown in Fig. 4. Depending on the capabilities of the robot, a safety check with the relation of the sole area A_{sole} and the supporting polygon area A_F

$$\frac{A_F}{A_{sole}} > \epsilon_A \tag{3}$$

where $\epsilon_A \in [0, 1]$ is a contact size ratio that can be used for deciding whether to step over an obstacle or take other action, for example, a step re-plan as in [14], or an emergency stop as in [21]. Once the ZMP reference positions are re-targeted, the motion for the CoM will be adapted naturally by most walking pattern generators such as the preview control [7] or the ZMP-DCM-CoM chained control [2].

A. Balance control using the contact geometry

A necessary condition for stable biped walking is the existence of the ZMP inside the supporting polygon [22]. Furthermore, if the ZMP gets too close to the edge, the robot can tilt at the slightest disturbance and fall. To prevent this, balance controllers push the ZMP away from the edges of the supporting polygon by distributing the contact forces along the sole.

Different strategies can be applied for balance control. For example, an efficient method is to use a feedback loop with the DCM to shift the desired position for the ZMP as proposed in [2]. This method can be complemented with plantar tactile feedback as follows.

The LIPM dynamics can be described as

$$\ddot{\boldsymbol{x}} = \omega^2 (\boldsymbol{x} - \boldsymbol{p}) \in \mathbb{R}^2, \tag{4}$$

where $\boldsymbol{x} = [x_x \; x_y \;]^\top \in \mathbb{R}^2$ is the position of the CoM, $\boldsymbol{p}$ is the ZMP, and $\omega = \sqrt{g/x_z}$ assuming a constant x_z. The DCM of the LIPM is defined as $\boldsymbol{\xi} = \boldsymbol{x} + \dot{\boldsymbol{x}}/\omega \in \mathbb{R}^2$, and it can help rewrite the LIPM model as

$$\dot{\boldsymbol{\xi}} = \omega (\boldsymbol{\xi} - \boldsymbol{p}) \tag{5}$$

$$\dot{\boldsymbol{x}} = \omega (\boldsymbol{\xi} - \boldsymbol{x}) . \tag{6}$$

The DCM is also used to generate a stable walking motion reference for the CoM $\boldsymbol{x}_d$ from reference ZMP way-points $\boldsymbol{p}_r$. The desired DCM trajectory $\boldsymbol{\xi}_d$ can be tracked defining the closed loop dynamics

$$\dot{\boldsymbol{\xi}} = \dot{\boldsymbol{\xi}}_d + k_\xi (\boldsymbol{\xi}_d - \boldsymbol{\xi}) \tag{7}$$

which combined with (5) and (6) can be used to adjust the reference ZMP $\boldsymbol{p}_r$ to a desired ZMP

$$\boldsymbol{p}_d = \boldsymbol{p}_r - \left(1 + \frac{k_\xi}{\omega}\right) (\boldsymbol{\xi}_d - \boldsymbol{\xi}) \tag{8}$$

which can be tracked by a ZMP feedback controller. Nevertheless, it must be guaranteed that $\boldsymbol{p}$ exists inside the supporting polygon to maintain stability. Therefore, its adjusted desired trajectory $\boldsymbol{p}_d$ must be constrained inside the estimated supporting polygon S_F as a safety measurement. Hence, after computing a first approximation $\boldsymbol{p}_{d,ini}$ two cases are possible as shown in Fig. 5. a) $\boldsymbol{p}_{d,ini}$ lays inside S_F and thus $\boldsymbol{p}_d = \boldsymbol{p}_{d,ini}$, b) $\boldsymbol{p}_{d,ini}$ lays outside S_F and must be shifted to the closest point in S_F. Algorithm 1 verifies the first case and applies the adjustment of the second case when needed from the vertices of S_F, and the initial adjusted ZMP reference $\boldsymbol{p}_{d,ini}$. As highlighted by Englsberger and Ott in [2], such projection of $\boldsymbol{p}_{d,ini}$ can produce discontinuities in the adjusted control signals. Furthermore, the online

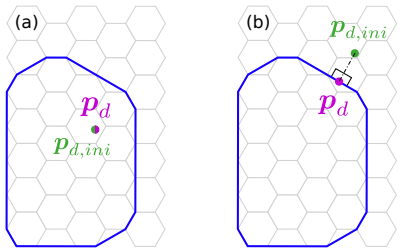

Fig. 5: Constraining the adjusted desired ZMP $\boldsymbol{p}_d$ to stay inside S_F with Algorithm 1.

adjustment of the supporting polygon and the re-targeting of $\boldsymbol{p}_r$ and the DCM waypoints also produce considerable discontinuities in the control signals. However, the enforcement of the contact constraints into the walking motions to prevent tilting is more important, and in practice, as will be shown in Section IV the desired trajectories or the CoM are smooth due to the chained dynamics of the ZMP-DCM-CoM system. Nevertheless, future works will address the discontinuities by adjusting the step time and generating smooth spline trajectories when motion re-targeting is triggered. Another possible improvement is to project $\boldsymbol{p}_d$ to the closest point in S_F that lays over the line that intersects $\boldsymbol{\xi}_d$ and $\boldsymbol{\xi}$. In practice, the closest point in S_F computed with Algorithm 1 is close enough to such line that the difference can be neglected (in the experiments shown in Section IV, it is always below 5 mm).

There are different methods for ZMP tracking. One useful example for position-controlled robot interfaces is by defining stable closed-loop dynamics, similar to Eq. (8) as

$$\dot{\boldsymbol{p}} - \dot{\boldsymbol{p}}_d = -k_p \left(\boldsymbol{p} - \boldsymbol{p}_d\right) \tag{9}$$

which can be derived and expanded to an adjusted reference for the CoM, considering $\dot{\boldsymbol{p}}_d = \dot{\boldsymbol{x}}_r - \frac{1}{\omega^2}\dddot{\boldsymbol{x}}_r$ with $\dddot{\boldsymbol{x}}_r = 0 \in \mathbb{R}^2$ a zero jerk reference trajectory for the CoM as

$$\dot{\boldsymbol{x}}_r = \dot{\boldsymbol{p}} + k_p(\boldsymbol{p} - \boldsymbol{p}_d) \tag{10}$$

which closes the loop, commanding the velocity of the CoM using ZMP feedback. Section IV will use this balance controller to walk over partial footholds.

B. Constrained contact wrench distribution

As reviewed in Section III-A, a common strategy for ZMP tracking is through CoM admittance control. However, plantar wrench control can improve the ZMP tracking by distributing the contact forces along the sole as proposed in [23]. Furthermore, if the contact area is smaller than the sole, such distribution of forces must be calculated within the contact geometry. Fortunately, the supporting polygon estimated by plantar skin can help define the constraints for different controllers. For example, adopting the contact stability formulation proposed by Caron et al. [6], which defines linear constraints for an ankle-wrench distribution QP from the supporting polygon assuming full-sole contacts. The formulation of these constraints is the contact wrench cone

Algorithm 1 Constraint $\boldsymbol{p}_d$ inside S_F

Require: S_k: the k vertices of S_F in clockwise order, $\boldsymbol{p}_{d,ini} \in \mathbb{R}^3, p_{d,ini,z} = 0$
Ensure: $\boldsymbol{p}_d \in S_F$ such that $||\boldsymbol{p}_d - \boldsymbol{p}_{d,ini}|| = \inf\{||a - \boldsymbol{p}_{d,ini}|| \mid a \in S_F\}$

```
Function next(j)
if j = k then
    return 1
else
    return j + 1
end if

p_d = S_k(1)
inside = true
for i = 1 to k do
    l = S_k(next(i)) − S_k(i)
    d = p_{d,ini} − S_k(i)
    v = d × l
    if v_z > 0 then
        r = (d · l) / (l · l)
        if r ≤ 0 then
            p̃_d = S_k(i)
        else if 0 < r < 1 then
            p̃_d = S_k(i) + r l
        else if 1 ≤ r then
            p̃_d = S_k(next(i))
        end if
        if ||p_{d,ini} − p̃_d|| < ||p_{d,ini} − p_d|| then
            p_d = p̃_d
        end if
        inside = false
    end if
end for
if inside then
    p_d = p_{d,ini}
end if
```

$$\begin{aligned}
|f_x| &\leq \mu f_z && (11)\\
|f_y| &\leq \mu f_z && (12)\\
f_z &> 0 && (13)\\
|\tau_x| &\leq Y f_z && (14)\\
|\tau_y| &\leq X f_z && (15)\\
\tau_{z,min} \leq \ & \tau_z \ \leq \tau_{z,max}, && (16)
\end{aligned}$$

where

$$\begin{aligned}
\tau_{z,min} &:= -\mu\,(X+Y)\,f_z + |Y f_x - \mu\tau_x| + |X f_y - \mu\tau_y|\\
\tau_{z,max} &:= +\mu\,(X+Y)\,f_z - |Y f_x + \mu\tau_x| - |X f_y + \mu\tau_y|
\end{aligned}$$

μ is the friction coefficient, and X, Y are the dimensions of the sole as shown in Fig. 6. Now, in the case of a partial foothold the wrench cone can be reshaped as follows.

Keeping the constraint that the contact is still an axis-aligned rectangle, optimization algorithms as [24] can construct this rectangle as the maximum area rectangle inscripted inside the supporting polygon, or merely as a bounding box of the contact with a safety inner offset. Note that the second is less accurate but faster to compute, and, therefore, would require a conservative margin to be applicable in realistic scenarios.

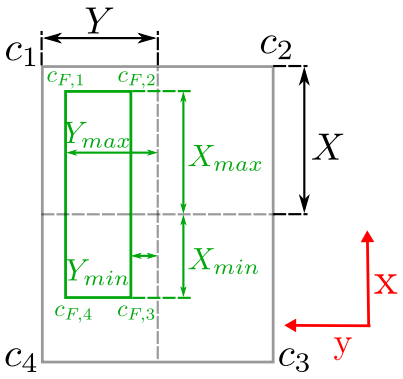

Fig. 6: Contact constraints geometry in [6] adapted to smaller rectangular contact areas approximated with plantar tactile feedback.

As shown in Fig. 6, the limits of the contact are now divided by maximum X_{max}, Y_{max} and minimum X_{min}, Y_{min} for each axis. With this geometry, the torsional part of the wrench cone (Eq. 14 and 15) is redefined as

$$Y_{max} f_z \leq \quad \tau_x \quad \leq Y_{min} f_z \tag{17}$$
$$X_{min} f_z \leq \quad \tau_y \quad \leq X_{max} f_z, \tag{18}$$

however, the constraints for τ_z (Eq. 16) can no longer be expressed in the concise notation and must consider the different cases

$$\begin{aligned}
-Y_{max} f_x - X_{max} f_y - \mu(X_{max} + Y_{max}) f_z + \mu\tau_x + \mu\tau_y &\leq \tau_z \\
-Y_{max} f_x + X_{min} f_y - \mu(X_{min} + Y_{max}) f_z + \mu\tau_x - \mu\tau_y &\leq \tau_z \\
+Y_{min} f_x - X_{max} f_y - \mu(X_{max} + Y_{min}) f_z - \mu\tau_x + \mu\tau_y &\leq \tau_z \\
+Y_{min} f_x + X_{min} f_y - \mu(X_{min} + Y_{min}) f_z - \mu\tau_x - \mu\tau_y &\leq \tau_z \\
-Y_{max} f_x - X_{max} f_y + \mu(X_{max} - Y_{max}) f_z - \mu\tau_x - \mu\tau_y &\geq \tau_z \\
-Y_{max} f_x + X_{min} f_y + \mu(X_{min} - Y_{max}) f_z - \mu\tau_x + \mu\tau_y &\geq \tau_z \\
+Y_{min} f_x - X_{max} f_y + \mu(X_{max} - Y_{min}) f_z + \mu\tau_x - \mu\tau_y &\geq \tau_z \\
+Y_{min} f_x + X_{min} f_y + \mu(X_{min} - Y_{min}) f_z + \mu\tau_x + \mu\tau_y &\geq \tau_z .
\end{aligned}$$

With these new constraints, the solution of the QP will generate an ankle wrench, which distributes the contact forces on the corners of the rectangle $c_{F,i}$ shown in Fig. 6.

IV. EXPERIMENTAL RESULTS

A. Experimental platforms

The adjustment of the ZMP reference to the centroid of the measured supporting polygon was tested in two robots running different walking controllers. a) the HRP-2 Kai robot with a total mass of 65 Kg running an LIPM tracking MPC based controller [1], and b) the H1 robot with a total mass of 86 Kg running the DCM-ZMP based controller [2]. The ZMP adjustment from the center of the supporting polygon was adapted without deep modifications in the structure of both controllers. Plantar skin was mounted on both robots, covering completely the soles. The skin used in the experiments is the latest version of [25]. The sensing system comprises a lattice array of hexagonal taxels (as shown in Fig. 2) with an apothem of 14.125 mm. Every taxel measures normal contact forces up to 300 N with a 12 bit resolution delivering the tactile information at 250 Hz.

The experiments presented in this section analyze the performance of the robots walking over obstacles with an area smaller than the foot sole. In every case,the robots are commanded to take six forward steps with no previous knowledge on the terrain. The step size is 20 cm, and the height of the swing foot motion is 8 cm. Early contacts are detected by the plantar skin, which triggers the stop of the swing foot motion. When the contact area is less than 90% of the sole (i.e. $\epsilon_A < 0.9$) the walking motion is adjusted to step over a partial foothold as described in the previous Sections. The robots are commanded to keep a height of 0.8 m during all the experiments.

B. Walking over partial footholds with constrained DCM-ZMP feedback control

The first experiments show the H1 robot walking over two different obstacles, one that required a ZMP adjustment in the sagittal plane and one in the frontal plane to challenge the versatility of the proposed methods. The single support time was $t_{ss} = 0.9$ [s], and the double support time $t_{ds} = 0.3$ [s].

In Fig. 7-(a,b,c), the foothold only covers the rear half of the robot sole. When the foot lands over the obstacle, the plantar skin approximates the shape of the contact, and the reference point for the ZMP $\boldsymbol{p}_r$ is shifted to the center of the reconstructed supporting polygon. The reference waypoints for the DCM $\boldsymbol{\xi}_r$ are updated too. While shifting the robot's weight to the new supporting foot, the balance controller shifts the desired ZMP $\boldsymbol{p}_d$ to track the new reference waypoints for the DCM $\boldsymbol{\xi}_r$. Nevertheless, the adjustment is constrained within the measured supporting polygon. Fig. 7-(d,e,f) shows a similar experiment with an obstacle that only covers 30% of the sole. In this case, the adjustment is performed in the y axis (in the frontal plane of the robot).

C. Walking over partial footholds with optimal contact stabilization

The next experiments show the HRP-2 Kai robot walking over two different obstacles, one that required a ZMP adjustment in the sagittal plane and one in the frontal plane to challenge the versatility of the proposed method. The single support time was assigned as $t_{ss} = 1.4$ [s], and the double support time as $t_{ds} = 0.5$ [s].

In Fig. 8-(a,b,c), the foothold only covers the rear half of the robot sole. When the foot lands over the obstacle, the plantar skin approximates the shape of the contact, and the reference point for the ZMP $\boldsymbol{p}_r$ is shifted to the center of the reconstructed supporting polygon. Then, the robot defines the contact constraints X_{max} and X_{min} from the maximum area rectangle inscribed in the supporting polygon. These limits define the constraints for the wrench distribution QP (Section II-C of [1]), which controls the real ZMP $\boldsymbol{p}$. A closer look at the constraint adjustment is detailed in Fig. 8-(c). The dashed green line is the original constraint X, which considers full-sole contact. Fig. 8-(d,e,f) shows a similar experiment with an obstacle that only covers around 2/3 of the sole from one side. In this case, the adjustment is performed in the y axis (in the frontal plane of the robot).

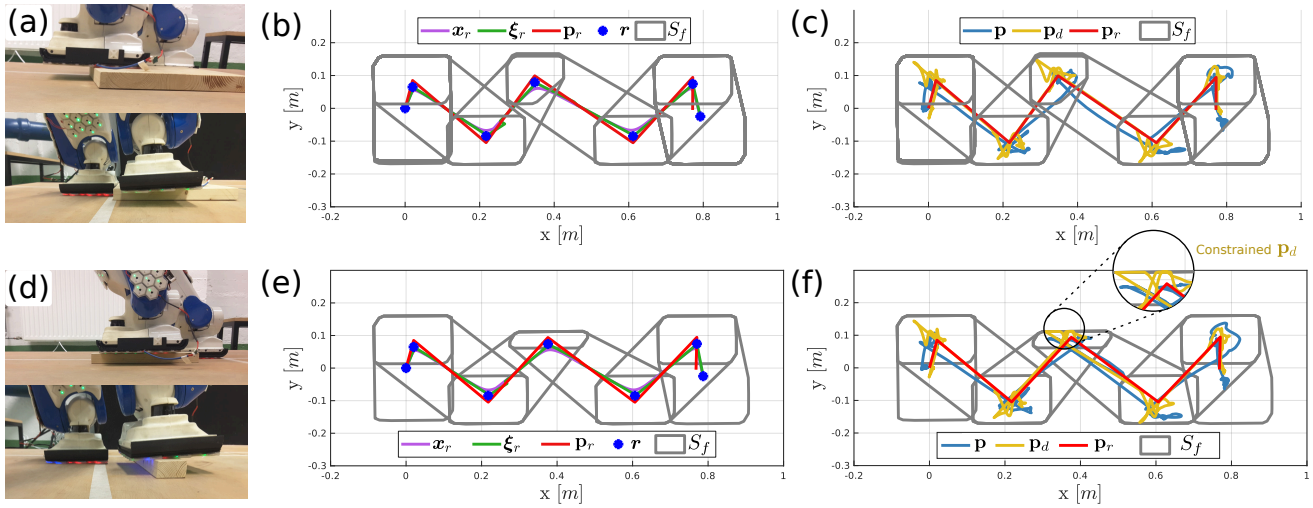

Fig. 7: The H1 robot walking over partial footholds. a) The first obstacle tested covers the rear half of the sole. b) shows the adjustment of the walking reference trajectories. c) shows the tracking of the ZMP constrained in the supporting region S_F. $\boldsymbol{r}$ are the VRP, $\boldsymbol{\xi}_r$ is the reference trajectory for the DCM, $\boldsymbol{x}_r$ is the reference trajectory for the CoM, $\boldsymbol{p}_r$ is the reference trajectory for the ZMP, $\boldsymbol{p}_d$ is the adjusted desired position of for the ZMP, and $\boldsymbol{p}$ is the real ZMP during the experiment. (d, e, f) show the second obstacle tested, a bar that covers only 30% of the sole.

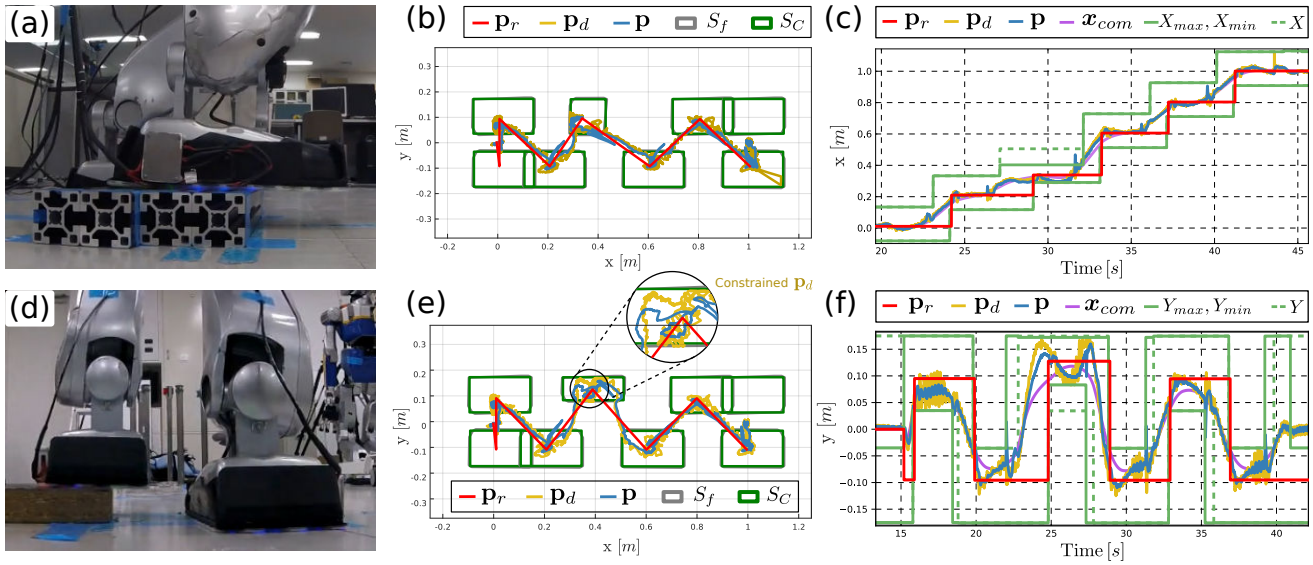

Fig. 8: The HRP-2 robot walks over obstacles that produce contacts smaller than the sole. The plantar skin approximates the supporting polygon S_F, and the contact constraints for the ZMP wrench distribution control are defined as the bounding box S_F with a safety inner offset of 1 cm. (a,b,c) the obstacle requires an adjustment in the sagittal direction. (c,d,e) The obstacle triggers an adjustment in the lateral direction. The reference ZMP $\boldsymbol{p}_r$ is shifted to the center of the contact area. The desired ZMP $\boldsymbol{p}_d$ is adjusted and constrained within the supporting area, and the real ZMP $\boldsymbol{p}$ is controlled to track $\boldsymbol{p}_d$ considering the hard constraints X_{max},X_{min}, Y_{max}, and Y_{min}.

V. CONCLUSION

In this work, a new scheme for enabling walking over partial footholds using plantar robot skin was proposed. The geometric information that tactile feedback provides helps adjust the walking motions right after landing a new step. The spatial distribution of contact force sensors provides an approximation of the shape of the foothold. With this information, a walking robot can construct the supporting polygon and use its centroid as the reference point for ZMP-DCM control. Furthermore, knowing the supporting polygon allows for defining constraints for optimal contact wrench stabilization.

These methods were tested in two robots that run walking controllers with different approaches. The H1 robot used a classic implementation with leg inverse kinematics for tracking the reference trajectories and ZMP control with only CoM motion adjustment. The HRP-2 Kai had a walking controller based on whole-body inverse kinematics with optimal

foot contact stabilization. Both controllers were designed to walk over flat terrain with the classic full-sole contact assumption. As shown in Section IV, both robots could step over small footholds, keeping the supporting contact stable. The situation where the partial foothold was on the tip of the foot produced ankle torques that were too high for both robots, leading to foot tilting due to motor tracking errors and overheating of the motors. Therefore, it is recommended to avoid partial footholds on the tip of the feet and keep them as close to the angle motors as possible.

The walking controllers used to assess the methods described in this work always keep a constant step time. This feature limits the capacity of a robot to react robustly to more complex terrain conditions. The shift of the target ZMP induces an effect similar to the step corrections based on step capturability [26]. The step time should be adjusted according to the new step length or the distance that the ZMP and DCM must traverse. Furthermore, the modifications in the contact constraints limit the amount of ankle torque the robot can exert on the ground. Thus, these constraints should also be considered when adjusting the walking motions. The step timing adjustment and a generalization of the constraint definition for arbitrary shapes will be assessed in future works.

VI. ACKNOWLEDGMENT

This work is a cooperation with the CNRS-AIST Joint Robotics Laboratory (JRL). Funded by the German Research Foundation (DFG) – 502086040, the Federal Ministry of Education and Research and the Free State of Bavaria under the Excellence Strategy of the Federal Government and the States supported by the Innovation Network eXprt of the Technical University of Munich. This result is part of a project that has received funding from the European Research Council (ERC) under the European Union's Horizon 2020 research and innovation programme (Grant agreement No. 101098308). Thanks to Arnaud Tanguy for his technical help.

REFERENCES

[1] S. Caron, A. Kheddar, and O. Tempier, "Stair climbing stabilization of the hrp-4 humanoid robot using whole-body admittance control," in *2019 International Conference on Robotics and Automation (ICRA)*, pp. 277–283, IEEE, 2019.

[2] J. Englsberger, C. Ott, M. A. Roa, A. Albu-Schäffer, and G. Hirzinger, "Bipedal walking control based on capture point dynamics," in *2011 IEEE/RSJ International Conference on Intelligent Robots and Systems*, pp. 4420–4427, IEEE, 2011.

[3] K. Kaneko, M. Morisawa, S. Kajita, S. Nakaoka, T. Sakaguchi, R. Cisneros, and F. Kanehiro, "Humanoid robot hrp-2kai—improvement of hrp-2 towards disaster response tasks," in *2015 IEEE-RAS 15th International Conference on Humanoid Robots (Humanoids)*, pp. 132–139, IEEE, 2015.

[4] E. Dean-Leon, J. R. Guadarrama-Olvera, F. Bergner, and G. Cheng, "Whole-body active compliance control for humanoid robots with robot skin," in *2019 International Conference on Robotics and Automation (ICRA)*, pp. 5404–5410, IEEE, 2019.

[5] J. Englsberger and C. Ott, "Integration of vertical com motion and angular momentum in an extended capture point tracking controller for bipedal walking," in *2012 12th IEEE-RAS International Conference on Humanoid Robots (Humanoids 2012)*, pp. 183–189, IEEE, 2012.

[6] S. Caron, Q.-C. Pham, and Y. Nakamura, "Stability of surface contacts for humanoid robots: Closed-form formulae of the contact wrench cone for rectangular support areas," in *2015 IEEE International Conference on Robotics and Automation (ICRA)*, pp. 5107–5112, IEEE, 2015.

[7] S. Kajita, F. Kanehiro, K. Kaneko, K. Fujiwara, K. Harada, K. Yokoi, and H. Hirukawa, "Biped walking pattern generation by using preview control of zero-moment point," in *2003 IEEE International Conference on Robotics and Automation (Cat. No. 03CH37422)*, vol. 2, pp. 1620–1626, IEEE, 2003.

[8] M. A. Hopkins, D. W. Hong, and A. Leonessa, "Humanoid locomotion on uneven terrain using the time-varying divergent component of motion," in *2014 ieee-ras international conference on humanoid robots*, pp. 266–272, IEEE, 2014.

[9] M. B. Popovic, A. Goswami, and H. Herr, "Ground reference points in legged locomotion: Definitions, biological trajectories and control implications," *The International Journal of Robotics Research*, vol. 24, no. 12, pp. 1013–1032, 2005.

[10] Y. Lee, H. Lee, S. Hwang, and J. Park, "Terrain edge detection for biped walking robots using active sensing with vcop-position hybrid control," *Robotics and Autonomous Systems*, vol. 96, pp. 41–57, 2017.

[11] G. Wiedebach, S. Bertrand, T. Wu, L. Fiorio, S. McCrory, R. Griffin, F. Nori, and J. Pratt, "Walking on partial footholds including line contacts with the humanoid robot atlas," in *Humanoid Robots (Humanoids), 2016 IEEE-RAS 16th International Conference on*, pp. 1312–1319, IEEE, 2016.

[12] R. J. Griffin, G. Wiedebach, S. McCrory, S. Bertrand, I. Lee, and J. Pratt, "Footstep planning for autonomous walking over rough terrain," in *2019 IEEE-RAS 19th International Conference on Humanoid Robots (Humanoids)*, pp. 9–16, IEEE, 2019.

[13] F. Sygulla and D. Rixen, "A force-control scheme for biped robots to walk over uneven terrain including partial footholds," *International Journal of Advanced Robotic Systems*, vol. 17, no. 1, p. 1729881419897472, 2020.

[14] J. Rogelio Guadarrama Olvera, E. D. Leon, F. Bergner, and G. Cheng, "Plantar tactile feedback for biped balance and locomotion on unknown terrain," *International Journal of Humanoid Robotics*, vol. 17, no. 01, p. 1950036, 2020.

[15] J. R. Guadarrama-Olvera, S. Kajita, and G. Cheng, "Preemptive foot compliance to lower impact during biped robot walking over unknown terrain," *IEEE Robotics and Automation Letters*, vol. 7, no. 3, pp. 8006–8011, 2022.

[16] J. L. Bentley, F. P. Preparata, and M. G. Faust, "Approximation algorithms for convex hulls," *Communications of the ACM*, vol. 25, no. 1, pp. 64–68, 1982.

[17] I. van der Hoog, V. Keikha, M. Löffler, A. Mohades, and J. Urhausen, "Maximum-area triangle in a convex polygon, revisited," *Information Processing Letters*, p. 105943, 2020.

[18] K. Jin and K. Matulef, "Finding the maximum area parallelogram in a convex polygon.," in *CCCG*, 2011.

[19] C. Schwarz, J. Teich, E. Welzl, and B. Evans, "On finding a minimal enclosing parallelogram," *International Computer Science Institute, Berkeley, CA, Tech. Rep. tr-94-036*, 1994.

[20] B. Khorshidi, "A new method for finding the center of gravity of polygons," *Journal of Geometry*, vol. 96, pp. 81–91, dec 2009.

[21] M. Morisawa, S. Kajita, K. Harada, K. Fujiwara, F. Kanehiro, K. Kaneko, and H. Hirukawa, "Emergency stop algorithm for walking humanoid robots," in *2005 IEEE/RSJ International Conference on Intelligent Robots and Systems*, pp. 2109–2115, IEEE, 2005.

[22] M. Vukobratović and J. Stepanenko, "On the stability of anthropomorphic systems," *Mathematical biosciences*, vol. 15, no. 1-2, pp. 1–37, 1972.

[23] S. Kajita, M. Morisawa, K. Miura, S. Nakaoka, K. Harada, K. Kaneko, F. Kanehiro, and K. Yokoi, "Biped walking stabilization based on linear inverted pendulum tracking," in *2010 IEEE/RSJ International Conference on Intelligent Robots and Systems*, pp. 4489–4496, IEEE, 2010.

[24] K. Daniels, V. Milenkovic, and D. Roth, "Finding the largest area axis-parallel rectangle in a polygon," *Computational Geometry*, vol. 7, no. 1-2, pp. 125–148, 1997.

[25] G. Cheng, E. Dean-Leon, F. Bergner, J. R. G. Olvera, Q. Leboutet, and P. Mittendorfer, "A comprehensive realization of robot skin: Sensors, sensing, control, and applications," *Proceedings of the IEEE*, vol. 107, no. 10, pp. 2034–2051, 2019.

[26] R. J. Griffin, G. Wiedebach, S. Bertrand, A. Leonessa, and J. Pratt, "Walking stabilization using step timing and location adjustment on the humanoid robot, atlas," in *2017 IEEE/RSJ International Conference on Intelligent Robots and Systems (IROS)*, pp. 667–673, IEEE, 2017.